Journal of Alloys and Compounds 509 (2011) 9050–9054

Contents lists available at ScienceDirect

Journal of Alloys and Compounds

journal homepage: www.elsevier.com/locate/jallcom

Magnetic, electrical and plastic properties of $Fe_{76}Nb_2Si_{13}B_9$, $Fe_{75}Ag_1Nb_2Si_{13}B_9$ and $Fe_{75}Cu_1Nb_2Si_{13}B_9$ amorphous alloys

Z. Stokłosa [a,*], J. Rasek [a], P. Kwapuliński [a], G. Badura [a], G. Haneczok [a], L. Pająk [a], J. Lelątko [a], A. Kolano-Burian [b]

[a] Institute of Material Science, University of Silesia, Bankowa 12, 40-007 Katowice, Poland
[b] Institute of Non-Ferrous Metals, Sowińskiego 5, 44-100 Gliwice, Poland

ARTICLE INFO

Article history:
Received 15 March 2011
Received in revised form 17 May 2011
Accepted 18 May 2011
Available online 29 June 2011

Keywords:
Amorphous alloys
Optimization effects
Magnetic losses
Plastic deformation

ABSTRACT

Influence of 1 h annealing in vacuum on magnetic, electrical and plastic properties of $Fe_{76}Nb_2Si_{13}B_9$, $Fe_{75}Ag_1Nb_2Si_{13}B_9$ and $Fe_{75}Cu_1Nb_2Si_{13}B_9$ melt spun ribbons were carefully investigated. It was shown that in all cases soft magnetic properties can be significantly enhanced by applying 1-h annealing at characteristic temperatures T_{op}. This optimization annealing causes that permeability increases more than 15-times and magnetic losses (tangent of loss angle) achieves a minimum in relation to the as quenched state. Using structural examinations (X-ray and HRTEM) it was shown that for the $Fe_{75}Cu_1Nb_2Si_{13}B_9$ alloy the optimized microstructure corresponds to a nanocrystalline αFe(Si) phase whereas in other alloys to a relaxed amorphous phase free of iron nanograins. As a consequence of this fact the $Fe_{76}Nb_2Si_{13}B_9$ and $Fe_{75}Ag_1Nb_2Si_{13}B_9$ alloys show higher plasticity in comparison to the nanocrystalline $Fe_{75}Cu_1Nb_2Si_{13}B_9$ alloy. Temperatures of the first stage of crystallization, and related diffusion parameters were determined using measurements of resistivity versus temperature with different heating rates.

1. Introduction

Amorphous alloys based on iron, obtained by melt spinning technique, for a suitable chemical compositions show very good soft magnetic, plastic and electrical properties [1]. From the economical point of view these alloys are considerably cheaper in relation to other type of amorphous alloys i.e. based on nickel or cobalt. Moreover magnetic properties of amorphous alloys based on iron can be enhanced by applying a preliminary thermal annealing usually called the optimization annealing [2–8]. The term enhancement in this context means a significant increase of magnetic permeability correlated with a decrease of magnetic losses.

In many papers it was shown that depending on chemical composition of an amorphous alloy and parameters of the applied annealing, the improvement of soft magnetic properties can be attributed to the so-called relaxed amorphous phase or to the nanocrystalline phase [1–12].

In the family of nanocrystalline alloys one can distinguish different groups of alloys with similar chemical composition i.e. *finemet* (Fe–Cu–Nb–Si–B) [13], *nanoperm* (Fe–Cu–Nb–Zr–Hf–B) [14] or *hitperm* (Fe–Co–Cu–Zr–Nb–Hf–B) [15–17]. Unfortunately, all the nanocrystalline alloys because of a fine-grained microstructure are relatively brittle and for this reason some difficulties in their industrial applications have been noticed. In this context the problem of alloy plasticity becomes an important question from both scientific and practical point of view. One of a possible way of improving alloy plasticity consists in selection of a suitable chemical composition ensuring that the optimized microstructure is free of iron nanograins and the enhancement of soft magnetic properties is due to formation of the relaxed amorphous phase [1–8,11,12]. In this case the main difficulty lies in thermal stability of the relaxed amorphous phase (see e.g. [18]) and as it was shown in [1,2,5] for melt spun ribbons such atoms as B, Si and also Nb play an important role in microstructure stabilization. The trick consists in slowing down of diffusion processes which shifts the nanocrystallization into higher temperatures and makes possible formation of the relatively stable relaxed amorphous phase.

The aim of the present paper is to examine the influence of thermal annealing on magnetic, electrical and plastic properties and crystallization of amorphous $Fe_{76}Nb_2Si_{13}B_9$, $Fe_{75}Ag_1Nb_2Si_{13}B_9$ and $Fe_{75}Cu_1Nb_2Si_{13}B_9$ alloys. In connection with this, it is worth to add that magnetic and electrical properties, as well as thermal properties of amorphous iron based alloys containing silver ($Fe_{75-x}Ag_xSi_9B_{16}$, free of Nb with $x = 0, 1, 2, 3, 4$) were investigated by Efthimiadis et al. [19] and Chrissaffis et al. [20], respectively.

2. Experimental procedure

The examined alloys i.e. $Fe_{76}Nb_2Si_{13}B_9$, $Fe_{75}Ag_1Nb_2Si_{13}B_9$ and $Fe_{75}Cu_1Nb_2Si_{13}B_9$ were obtained by melt spinning technique in the form of strips with thickness and width of about 20 μm and 1 cm, respectively. As received material

* Corresponding author. Tel.: +48 32 3591554; fax: +48 32 2596929.
E-mail address: stoklosa@us.edu.pl (Z. Stokłosa).

0925-8388/$ – see front matter © 2011 Elsevier B.V. All rights reserved.
doi:10.1016/j.jallcom.2011.05.070

was annealed in vacuum for 1 h at temperature T_a ranging from 300 K to 800 K (step 25 K). For the annealed samples the following magnetic properties were measured at room temperature by applying RLC meter (Hewlet-Packard 4284A, magnetic field 0.5 A/m, frequency 1030 Hz): (i) initial relative magnetic permeability μ_r, (ii) intensity of magnetic relaxation (magnetic after-effects) $\Delta\mu_r/\mu_r$(where $\Delta\mu_r/\mu_r(t_1) - \mu_r(t_2)$,$t_1$ = 0.5 min. and t_2 min. after demagnetization), (iii) tangent of total magnetic loss angle tg δ. Parallel magnetostriction coefficient $\lambda_{s||}$ at saturation magnetic field was measured by Joule method (dilatometer with infrared sensor working with a resolution of about 10 nm). Plastic deformation $\varepsilon = d/2r$ (where d is the ribbon thickness and r is the bending radius corresponding to formation of the first brittle cracks) was measured in order to characterize the material brittleness [21,22]. Magnetization curves $B = B(H)$ and $\mu_r = \mu_r(H)$ were measured by applying Lake Shore fluxmeter.

For samples in the as quenched state magnetization M (at magnetic field 0.5 T) versus temperature was measured with heating rate 5 K/min by making use of magnetic balance technique. The Curie temperatures of all the examined alloys were determined from the inflection point of $M(T)$ curves. In addition magnetization in saturation at magnetic field 7 T was determined at temperatures 10 K and 300 K using magnetometer PPMS-7 (Quantum Design).

Kinetic of the first stage of crystallization was examined by applying resistivity versus temperature measurements (four point probe) carried out with different heating rates ranging from 0.5 K/min to 10 K/min. The parameters of the Arrhenius relation for the first stage of nanocrystallization (activation energy E_x and preexponential factor K_0) were determined using the Kissinger method [20,23]. In addition based on these measurements the resistivity temperature coefficient $\alpha_{300\,K}$ at 300 K was also determined.

Structural changes taking place in the annealed samples were examined by applying X-ray methods (Philips difractomter X'Pert PW 304060) and high resolution transmission electron microscope (JEM 3010B).

3. Results

The influence of 1-h annealing on physical properties of the $Fe_{75}Ag_1Nb_2Si_{13}B_9$ alloy is presented in Fig. 1 where different quantities measured at room temperature for annealed samples are plotted versus the annealing temperature T_a. So, Fig. 1a shows initial relative magnetic permeability $\mu_r(T_a)$ and tangent of magnetic loss angle tg δ(T_a), Fig. 1b shows electrical resistivity $\rho(T_a)$ and plastic deformation $\varepsilon(T_a)$, and finally, Fig. 1c shows intensity of magnetic relaxation $\Delta\mu_r/\mu_r$, and parallel magnetostricton coefficient $\lambda_{s||}$. One can see that the curve $\mu_r = \mu_r(T_a)$ exhibits relatively sharp maximum at a certain annealing temperature – denoted as T_{op} (optimization annealing) – which means that 1-h annealing at this temperature causes the strongest enhancement of soft magnetic properties of the examined alloy. Note, the temperature T_{op} and the value of permeability at maximum $\mu_r(T_{op})$ strongly depend on chemical composition of the studied alloy that will be commented in the next section. Comparing the curves $\mu_r = \mu_r(T_a)$ and tg δ = tg $\delta(T_a)$ one can notice that the maximum of permeability is correlated with the minimum of magnetic losses as it should be expected for the optimization annealing. Indeed, annealing at T_{op} reduces also the intensity of magnetic relaxation $\Delta\mu_r/\mu_r$ which means that thermal/time instabilities characteristic for the as quench state, after annealing at T_{op}, practically disappears. According to [24] the intensity $\Delta\mu_r/\mu_r$ can be connected with migration of atomic pairs in the vicinity of free volumes (microvoids). Taking into account this fact and data presented in Fig. 1 one can conclude that annealing out of free volume frozen into material during fabrication leads to a reduction of magnetic losses and intensity of magnetic relaxation.

Fig. 2 shows three curves of resistivity ρ measured versus temperature with heating rate 0.5 K/min for the $Fe_{76}Nb_2Si_{13}B_9$, $Fe_{75}Ag_1Nb_2Si_{13}B_9$ and $Fe_{75}Cu_1Nb_2Si_{13}B_9$ amorphous alloys. Initially, ρ increases with increasing temperature due to electron-phonon scattering in amorphous structure. At higher temperatures an abrupt drop of resistivity is observed which is surely related to the first stage of crystallization. An arbitrary taken condition $d\rho/dT = 0$ allows defining the so-called crystallization temperature T_x which depends on heating rate, as it should be expected for any diffusion controlled process. Based on this dependence and using the Kissinger method one can determine the parameters of the Arrhenius relation – the activation energy E_{x1} and the preexponential factor K_{01} for the first stage of crystallization i.e. for formation of the nanocrystalline phase αFe(Si). For the examined alloys, i.e. for the $Fe_{76}Nb_2Si_{13}B_9$, $Fe_{75}Ag_1Nb_2Si_{13}B_9$ and $Fe_{75}Cu_1Nb_2Si_{13}B_9$ we have obtained: $E_{x1} = 3.29 \pm 0.05$ eV, $E_{x1} = 3.25 \pm 0.05$ eV, $E_{x1} = 2.94 \pm 0.05$ eV, and $K_{01} = 7.4 \times 10^{17\pm2}\ s^{-1}$, $K_{01} = 7.3 \times 10^{17\pm2}\ s^{-1}$, $K_{01} = 6.6 \times 10^{17\pm2}\ s^{-1}$, respectively.

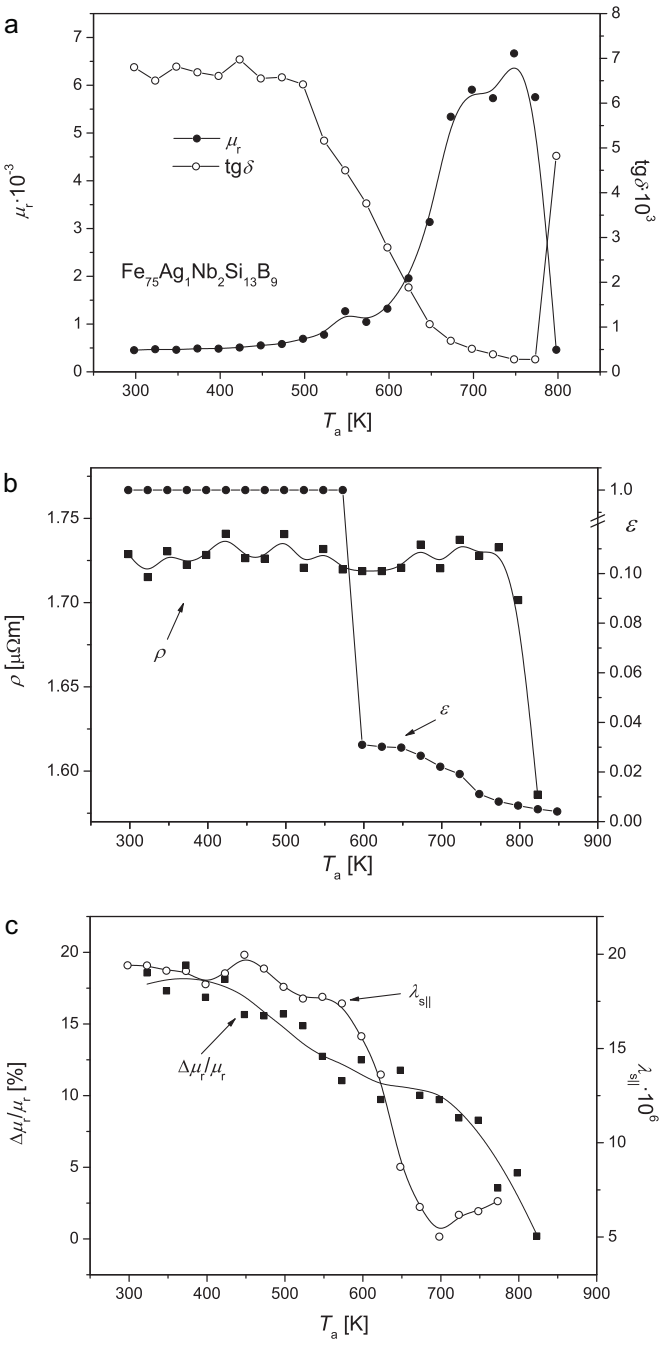

Fig. 1. Different physical properties measured at room temperature for annealed samples (for 1-h at T_a of the $Fe_{75}Ag_1Nb_2Si_{13}B_9$ alloy plotted versus the annealing temperature T_a; (a) initial magnetic permeability (field 0.5 A/m) and tangent of total magnetic loss angle, (b) electrical resistivity ρ and plastic deformation for bending ε, (c) intensity of magnetic relaxation $\Delta\mu_r/\mu_r$ and parallel magnetostricton coefficient $\lambda_{s||}$ at saturation field.

Fig. 3 shows the normalized magnetization in saturation $M(T)/M(300\,K)$ versus temperature measured at magnetic field 0.5 T and heating rate 5 K/min for the $Fe_{76}Nb_2Si_{13}B_9$, $Fe_{75}Ag_1Nb_2Si_{13}B_9$ and $Fe_{75}Cu_1Nb_2Si_{13}B_9$ alloys. In the tempera-

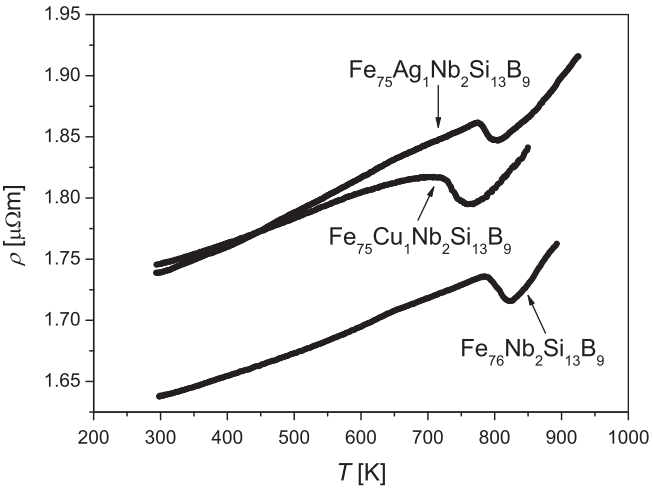

Fig. 2. Resistivity versus temperature for different amorphous alloys measured with heating rate 0.5 K/min.

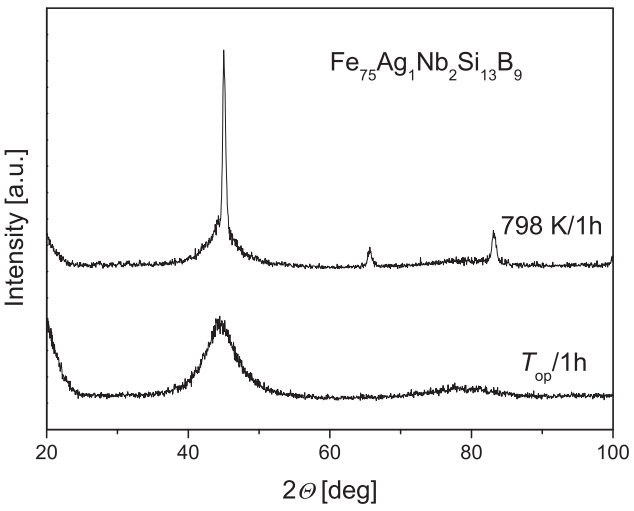

Fig. 4. X-ray diffraction patterns for the $Fe_{75}Ag_1Nb_2Si_{13}B_9$ alloy after the optimization annealing at temperature T_{op} and after annealing at 798 K/1 h.

ture range 300 K < T < 700 K (region a) magnetization monotonically decreases up to the Curie temperature of amorphous phase. The values of T_c, for all examined alloys, were determined from the inflection point of $M(T)$ curve which is a commonly used procedure. In the temperature range T_c < T < 800 K (region b) the examined sample is in paramagnetic state with almost zero magnetization. At higher temperatures i.e. 800 K < T < 850 K (region c) magnetization increases due to formation of nanocrystalline phase αFe(Si) for which the Curie temperature is above 1000 K. In this region one can also determine the crystallization temperature T_{x1} for the heating rate 5 K/min. At temperatures above 850 K (region d) magnetization decreases as it is expected for the crystalline phase with the Curie temperature of about 1030 K.

Fig. 4 shows two X-ray diffraction patterns obtained for sample of the $Fe_{75}Ag_1Nb_2Si_{13}B_9$ alloy annealed for 1-h at temperature $T_\alpha = T_{op}$ 748 K and at 798 K i.e. above T_{op}. One can conclude that after the optimization annealing the examined sample is in the relaxed amorphous state i.e. in amorphous state in which free volume (microvoids) content, in relation to the as quenched state, is significantly reduced. Such a reduction of free volume content is demonstrated in Fig. 1c where the intensity of magnetic relaxation $\Delta\mu_r/\mu_r$ is plotted versus T_a. The optimized microstructure (sample annealed at T_{op}/1 h) is shown in Fig. 5a and the corresponding diffraction pattern is presented in Fig. 5b. From Fig. 5 one can

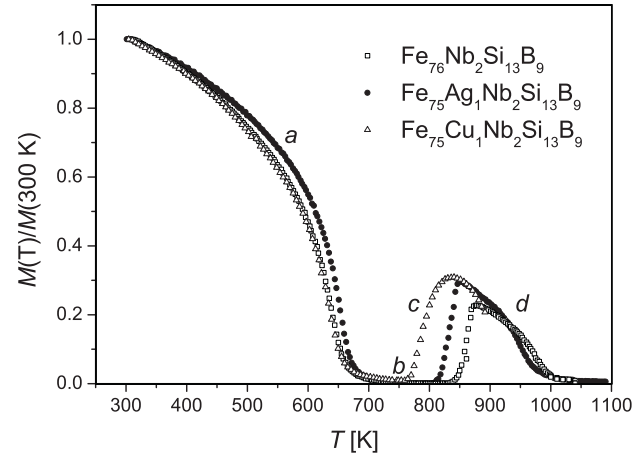

Fig. 3. Normalized magnetization at magnetic field 0.5 T versus temperature measured with heating rate 5 K/min.

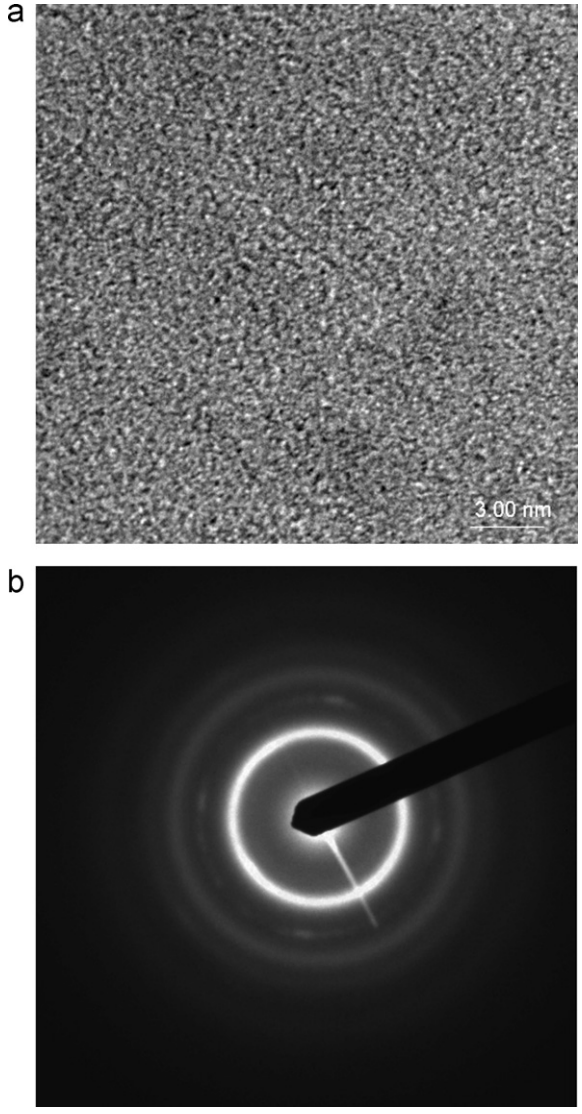

Fig. 5. HREM image (a) and electron diffraction pattern (b) for the $Fe_{75}Ag_1Nb_2Si_{13}B_9$ after annealing at temperature T_{op}.

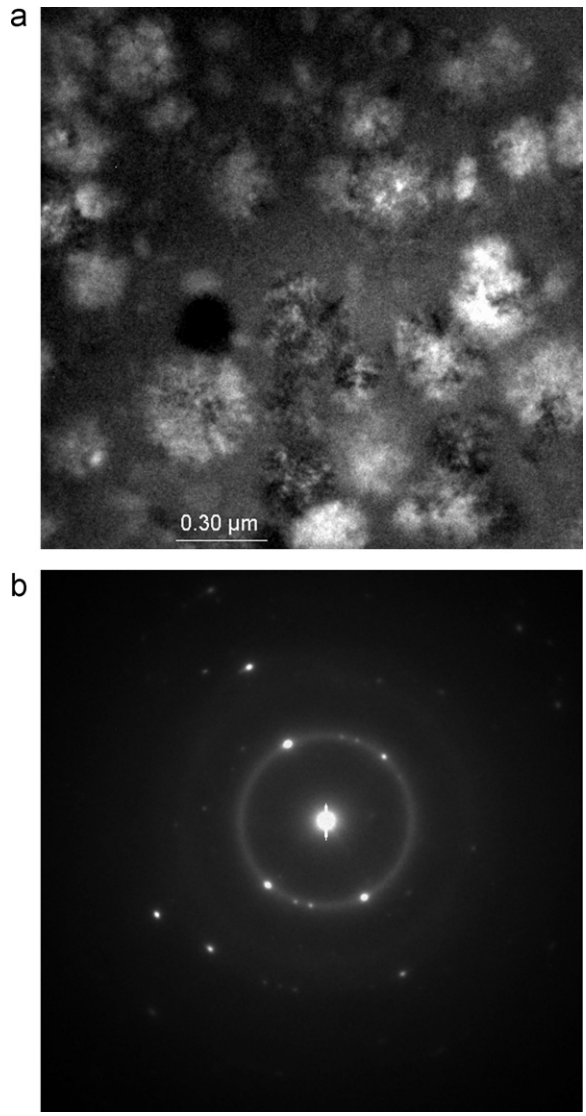

Fig. 6. TEM image (a) and electron diffraction pattern (b) for the $Fe_{75}Ag_1Nb_2Si_{13}B_9$ alloy after annealing at T_a = 798 K/1 h.

conclude again that the examined sample is in the relaxed amorphous state (free of iron nanograins). Fig. 6 shows microstructure and the corresponding diffraction pattern obtained for sample of the $Fe_{75}Ag_1Nb_2Si_{13}B_9$ alloy after annealing for 1-h at temperature T_a = 798 K. It is clear that 1-h annealing at temperature 50 K above causes formation of the nanocrystalline phase αFe(Si).

All the determined parameters characterizing different properties of the examined alloys are listed in Table 1.

4. Discussion

The data presented in preceding section (Fig. 1, and Table 1) show that soft magnetic properties of the $Fe_{76}Nb_2Si_{13}B_9$, $Fe_{75}Ag_1Nb_2Si_{13}B_9$ and $Fe_{75}Cu_1Nb_2Si_{13}B_9$ amorphous alloys can be significantly enhanced by applying a suitable 1-h annealing at temperature T_{op} listed in Table 1. It has to be stressed that after the optimization annealing magnetic permeability increases more than 15 times and tangent of magnetic loss angle decreases more than 1.5 times.

Structural examinations carried out for that $Fe_{76}Nb_2Si_{13}B_9$ and $Fe_{75}Ag_1Nb_2Si_{13}B_9$ alloys show that the optimized microstructure is free of iron nanograins which means that the observed enhancement can be attributed to formation of the relaxed amorphous phase. In this phase, as it was discussed in [1–8,11,12,18] the free volume (microvoids) content in relation to the as quenched state is significantly reduced. In our case it results from the data presented in Fig. 1 and Table 1. Indeed, the optimization annealing causes that the intensity of magnetic relaxation $\Delta\mu_r/\mu_r$ decreases at least 2-times. According to Kronmüller [24,25] the quantity $\Delta\mu_r/\mu_r$ depends on diffusion of atomic pairs in the vicinity of free volume. In the as quenched state this kind of diffusion plays a dominant role and leads to the known thermal/time instabilities of different physical properties sensitive to some micro-structural changes. Due to the optimization annealing free volume content is reduced, the diffusion is at least partially blocked and the stabilization energy drops down [1–8,11,12,24,25]. All these factors lead to an increase of magnetic permeability, a decrease of magnetic losses and improve thermal stability of the examined material.

Table 1
Curie temperatures T_c, temperatures of the first stage of crystallization T_{x1}, temperatures of the 1-h optimization annealing T_{op}, parameters of the Arrhenius relation of the first stage of crystallization E_{x1},K_{01}, resistivity at 300 K $\rho_{300\,K}$ and temperature coefficient of resistivity at 300 K $\alpha_{300\,K}$, plastic deformation ε, tangent of magnetic loss angle tg δ, magnetostriction coefficient $\lambda_{s||}$, intensity of magnetic relaxation $\Delta\mu_r/\mu_r$, initial magnetic permeability μ_r, magnetization in saturation at 10 K $\mu_0 M_{10\,K}$, and at 300 K $\mu_0 M_{300\,K}$; (RA, relaxed amorphous phase; N, nanocrystalline phase; asq, as quenched state; opt, optimized state).

Physical quantity	Material		
	$Fe_{76}Nb_2Si_{13}B_9$	$Fe_{75}Ag_1Nb_2Si_{13}B_9$	$Fe_{75}Cu_1Nb_2Si_{13}B_9$
Phase	RA	RA	N
T_c (K)	635	650	636
T_{X1} (K)	784	773	705
T_{op} (K)	673	748	823
$\mu_0 M_{10\,K}$ (T)	1.37	1.40	1.51
$\mu_0 M_{300\,K}$ (T)	1.20	1.26	1.31
$\rho_{300\,K}$ (μΩm)	1.63	1.74	1.75
$\alpha_{300\,K} \times 10^{-5}$ K^{-1}	11.6	11.9	7.4
ε^{asq}	1.0	1.0	0.03257
ε^{opt}	0.0205	0.0081	0.0049
tg δ^{asq}	0.0175	0.0068	0.0154
tg δ^{opt}	0.0119	0.0003	0.0090
$\lambda_{s\|\|}^{asq} \times 10^6$	18.6	19.4	12
$\lambda_{s\|\|}^{opt} \times 10^6$	5.8	6.9	0.5
$(\Delta\mu_r/\mu_r)^{asq}$ (%)	13.6	17.5	25
$(\Delta\mu_r/\mu_r)^{opt}$ (%)	6.1	3.5	1.2
μ_r^{asq}	320	450	500
μ_r^{opt}	6500	6700	9300
E_{x1} (eV)	3.29 ± 0.05	3.25 ± 0.05	2.94 ± 0.05
K_{01} (s^{-1})	$7.4 \times 10^{17\pm2}$	$7.3 \times 10^{17\pm2}$	$6.6 \times 10^{17\pm2}$

An addition of about 2 at% of Nb in $Fe_{78}Si_{13}B_9$ amorphous alloy cause an increase of temperature of the first stage of crystallization T_{x1} by 83 K and T_{op} by 50 K. The Curie temperature decreases by 29 K [2]. This facts show that Nb atoms cause a slowing down of diffusion processes in amorphous materials. On the contrary, an addition of 1 at% of copper in the $Fe_{76}Nb_2Si_{13}B_9$ alloy accelerates diffusion processes and the first stage of crystallization is shifted into lower temperatures. In relation to the copper free alloy the temperature T_{x1} for the $Fe_{75}Cu_1Nb_2Si_{13}B_9$ alloy is lower by about 80 K whereas the temperature T_{op} is higher by about 150 K. An addition of 1 at% Ag instead of Cu causes, in relation to the $Fe_{76}Nb_2Si_{13}B_9$ alloy, a decrease of T_x but only by about 10 K and an increase of T_{op} by about 50 K. Let notice (see Table 1) that for the nanocrystalline $Fe_{75}Cu_1Nb_2Si_{13}B_9$ alloy due to optimization annealing magnetic permeability increases about 18 times and tangent of magnetic loss angle decreases about 1.7 times.

It is known that for magnetic materials magnetization processes and what follows magnetic permeability depends on different kinds of internal energy like magnetoelastic, stabilization or magnetocrystalline energy and also on the value of magnetization in saturation [9,10,25–28].

The magnetoelastic energy depends on magnetostriction coefficients and the value of internal stresses. In amorphous alloys in the as quenched state the parallel magnetostriction coefficient $\lambda_{s||}$ in saturation magnetic field is much higher than after the optimization annealing at T_{op} (see Table 1). This means that such annealing reduces significantly the magnetoelastic energy and thereby causes an increase of magnetic permeability.

The stabilization energy, especially important for melt spun ribbons, is connected with the presence of free volume frozen into material during fabrication. This energy, directly proportional to the content of relaxing objects (e.g. atomic pairs in the vicinity of free volume) results from interaction of magnetic moment of relaxing object and spontaneous magnetization [29]. It is obvious that any annealing leading to a reduction of free volumes content causes at the same time a decrease of the stabilization energy. In particular this effect is observed after annealing at T_{op}, because the intensity of magnetic relaxation monitored as $\Delta\mu_r/\mu_r$ drops down. Moreover one can notice that this annealing causes an increase of magnetization in saturation in relation to the as quenched state. Consequently, due to annealing out of free volume magnetization processes proceed easier and magnetic permeability increases.

The magnetocrystalline energy in nanocrystalline alloys depends on the effective anisotropy constant $\bar{K}$ and this quantity strongly depends on amount of the formed nanocrystalline phase, the mean grain size and the length of ferromagnetic exchange interaction [9,10]. Hence, $\bar{K}$ for nanocrystalline material should be much lower than for the amorphous one because a system of randomly oriented grains averages out the anisotropy to almost zero value.

Finally, one can be concluded that for $Fe_{76}Nb_2Si_{13}B_9$, $Fe_{75}Ag_1Nb_2Si_{13}B_9$ alloys (the optimized microstructure corresponds to the relaxed amorphous phase) magnetic permeability depends on magnetoelastic energy, the stabilization energy and the value of magnetization in saturation. In the case of $Fe_{75}Cu_1Nb_2Si_{13}B_9$ alloy (the optimization microstructure correspond to the nanocrystalline phase) μ_r additionally depends on the effective magnetocrystalline energy.

Brittleness of the examined alloys can be evaluated by taking into account the plastic deformation $\varepsilon = d/2r$ (where d is the ribbon thickness and r is the bending radius for which the first brittle cracks are observed) measured as a parameter sensitive to formation of brittle cracks. It is obvious that an undesirable decrease of deformation ε, defined as above, corresponds to an increase of material brittleness. According to the data presented in Fig. 1 and Table 1 the $Fe_{75}Cu_1Nb_2Si_{13}B_9$ nanocrystalline alloy in the as quenched state is more brittle than the other examined alloys i.e. $Fe_{76}Nb_2Si_{13}B_9$ and $Fe_{75}Ag_1Nb_2Si_{13}B_9$. The same conclusion is valid for the optimized alloys i.e. ε^{opt} for the $Fe_{75}Cu_1Nb_2Si_{13}B_9$ alloy which is 0.005 is much lower than determined for the $Fe_{76}Nb_2Si_{13}B_9$ and $Fe_{75}Ag_1Nb_2Si_{13}B_9$ alloys. This means that addition of 1 at% of silver instead of copper essentially improves material plasticity.

5. Conclusions

1. Soft magnetic properties of the $Fe_{76}Nb_2Si_{13}B_9$, $Fe_{75}Ag_1Nb_2Si_{13}B_9$ and $Fe_{75}Cu_1Nb_2Si_{13}B_9$ amorphous alloys obtained by melt spinning technique can be significantly enhanced by applying 1-h annealing at temperatures T_{op} (see Table 1).
2. In amorphous alloys $Fe_{76}Nb_2Si_{13}B_9$, and $Fe_{75}Ag_1Nb_2Si_{13}B_9$ the optimized microstructure corresponds to the relaxed amorphous phase, whereas for the $Fe_{75}Cu_1Nb_2Si_{13}B_9$ alloy the optimized microstructure corresponds to the nanocrystalline phase αFe(Si).
3. The examined alloys $Fe_{76}Nb_2Si_{13}B_9$, and $Fe_{75}Ag_1Nb_2Si_{13}B_9$ in the as quenched state and after the optimization annealing show higher plasticity than the $Fe_{75}Cu_1Nb_2Si_{13}B_9$ alloy in the as quenched state and in the optimized state, respectively.

Acknowledgements

This work was supported by the Polish Ministry of Science and High School under grant No. NN 507460633.

References

[1] Z. Stokłosa, P. Kwapuliński, J. Rasek, G. Badura, G. Haneczok, L. Pająk, A. Kolano-Burian, J. Alloys Compd. 507 (2010) 465–469.
[2] G. Badura, J. Rasek, Z. Stokłosa, P. Kwapuliński, G. Haneczok, J. Lelątko, L. Pająk, J. Alloys Compd. 436 (2007) 43–50.
[3] Z. Stokłosa, J. Rasek, P. Kwapuliński, G. Haneczok, A. Chrobak, J. Lelątko, L. Pająk, Phys. Status Solidi A 207 (2010) 452–456.
[4] G. Haneczok, J. Rasek, Defect and Diffusion Forum 224–225 (2004) 13–26.
[5] G. Haneczok, J.E. Frąckowiak, A. Chrobak, P. Kwapuliński, J. Rasek, Phys. Status Solidi A 202 (2005) 2574–2581.
[6] A. Chrobak, G. Haneczok, P. Kwapuliński, D. Chrobak, Z. Stokłosa, J. Rasek, J. Alloys Compd. 423 (2006) 77–80.
[7] P. Kwapuliński, Z. Stokłosa, J. Rasek, G. Badura, G. Haneczok, L. Pająk, J. Lelątko, J. Magn. Magn. Mater. 320 (2008) e778–e782.
[8] J. Rasek, Z. Stokłosa, Eng. Trans. 54 (2006) 51–69.
[9] G. Herzer, L.L. Varga, J. Magn. Magn. Mater. 215–216 (2000) 506–512.
[10] G. Herzer, J. Magn. Magn. Mater. 294 (2005) 99–106.
[11] T. Naohara, Philos. Mag. Lett. 78 (1998) 229–234.
[12] T. Naohara, Philos. Mag. Lett. 78 (1998) 235–239.
[13] Y. Yoshizawa, S. Oguma, K. Yamauchi, J. Appl. Phys. 64 (1988) 6044–6046.
[14] A. Makino, T. Hatanai, Y. Naitoh, T. Bitoh, A. Inoue, IEEE Trans. Magn. 33 (1997) 3793–3798.
[15] X. Liang, T. Kulik, J. Ferenc, B. Xu, J. Magn. Magn. Mater. 308 (2007) 227–232.
[16] J. Zbroszczyk, A. Młynczyk, J. Olszewski, W. Ciurzyńska, M. Hasiak, R. Kolano, J. Lelątko, J. Magn. Magn. Mater. 304 (2006) e727–e729.
[17] R. Hasegawa, J. Magn. Magn. Mater. 304 (2006) 187–191.
[18] Ł. Madej, G. Haneczok, A. Chrobak, P. Kwapuliński, Z. Stokłosa, J. Rasek, J. Magn. Magn. Mater. 320 (2008) e774–e777.
[19] K.G. Efthimiadis, S.C. Chadjivasiliou, K.G. Melidis, A. Tsoukalas, J. Mater. Sci. 35 (2000) 2525–2528.
[20] K. Chrissaffis, Thermochim. Acta 411 (2004) 7–11.
[21] H. Chiriac, C. Hison, J. Magn. Magn. Mater. 254–255 (2003) 475–476.
[22] G. Kumar, M. Oknuma, T. Furubashi, T. Ohkubo, K. Hono, J. Non-Crystal. Solids 354 (2008) 882–888.
[23] F. Liu, X.N. Liu, O. Wang, J. Alloys Compd. 473 (2009) 152–156.
[24] H. Kronmüller, Philos. Mag. B 48 (1983) 127–150.
[25] H. Kronmüller, J. Magn. Magn. Mater. 140–144 (1995) 25–28.
[26] M. Rossignoll, Irreversibility of magnetization processes and hysteresis in real ferromagnetic materials, the role of defects , in: E. du Tremolet de Lacheisserie, D. Gignoux, M. Schlenker (Eds.), Magnetism Fundamentals, Springer, USA, 2005, pp. 209–247.
[27] R.C. O'Handley, Modern Magnetic Materials Principles and Applications , John Wiley and Sons, Inc., New York, 2000.
[28] A.H. Morish, The Physical Principles of Magnetism , John Wiley and Sons, Inc., New York, 2001.
[29] H. Kronmüller, J. Magn. Magn. Mater. 24 (1981) 159–167.